Biophysical Journal Volume 100 January 2011 489–497

Force Spectroscopy of Substrate Molecules En Route to the Proteasome's Active Sites

Mirjam Classen, Sarah Breuer, Wolfgang Baumeister,* Reinhard Guckenberger, and Susanne Witt*
Department of Molecular Structural Biology, Max Planck Institute of Biochemistry, Martinsried, Germany

ABSTRACT We used an atomic force microscope to study the mechanism underlying the translocation of substrate molecules inside the proteasome. Our specific experimental setup allowed us to measure interaction forces between the 20S proteasome and its substrates. The substrate (β-casein) was covalently bound either via a thiol-Au bond or by a PEG-based binding procedure to the atomic force microscope cantilever tip and offered as bait to proteasomes from *Methanosarcina mazei*. The proteasomes were immobilized densely in an upright orientation on mica, which made their upper pores accessible for substrates to enter. Besides performing conventional single-molecule force spectroscopy experiments, we developed a three-step procedure that allows the detection of specific proteasome-substrate single-molecule events without tip-sample contact. Using the active 20S wild type and an inactive active-site mutant, as well as two casein mutants bound with opposite termini to the microscope tip, we detected no directional preference of the proteasome-substrate interactions. By comparing the distribution of the measured forces for the proteasome-substrate interactions, were observed that a significant proportion of interaction events occurred at higher forces for the active versus the inactive proteasome. These forces can be attributed to the translocation of substrate en route to the active sites that are harbored deep inside the proteasome.

INTRODUCTION

The 20S proteasome is the 700 kDa, multisubunit, ATP-independent core protease of the eukaryotic 26S proteasome (1–4). The barrel-shaped architecture of the 20S proteasome is highly conserved from archaea to humans and is built of 14 α- and 14 β-subunits that are arranged in four heptameric rings in a $\alpha_7\beta_7\beta_7\alpha_7$ fashion. The interior of the 20S proteasome harbors a system of two antechambers and a central chamber that are connected by a channel that traverses the proteasome from one end to the other. Access to the interior of the complex is controlled by a gate in the α-subunit rings (5,6). The N-termini of the β-subunits form the single-residue active sites, which are sequestered from the cellular environment in the central chamber. Although exceptions have been reported (7), it is widely accepted that 20S proteasomes degrade substrates in a processive manner (8). It appears that the probability of an individual bond in a substrate to be cleaved increases with the mean residence time of the substrate in the vicinity of the active sites (9). It is likely that local structures near the active sites, and their interactions with the substrates, play a critical role in controlling the mean residence time (10,11).

The 20S proteasome is the prototype of a self-compartmentalizing molecular machine (12). The stratagem of self-compartmentalization allows potentially hazardous reactions, such as protein degradation, to take place amid the crowded molecular environment of cells by controlling access to the interior of the machines, where the reactions take place. The uptake of substrate molecules by the 20S proteasomes involves several steps: First, the substrates must be recognized by means of suitable cues, such as ubiqitin. They must then be unfolded for passage through the gates in the α-rings, a task performed by ATP-dependent regulatory complexes that bind to the α-rings of the 20S core complex. Finally, the substrates must wind their way through the system of internal cavities to reach the active sites located in the central chamber. Although the structure and enzymatic mechanism of the 20S proteasome have been elucidated in great detail, little is known about the mechanism underlying substrate translocation inside the proteasome. On the basis of in vitro data for (poly)peptide degradation, theoretical models have been developed to predict or rationalize the modes and kinetics of substrate cleavage inside 20S proteasomes (13–17). In modeling studies, the proteasome is assumed to be essentially a hollow cylinder that is accessible via two small openings; the specific molecular architecture of the proteasome's interior is not taken into account. In experimental attempts to reveal the mechanism of substrate translocation, it is usually difficult to separate the process of translocation from the process of substrate cleavage.

Here we report on atomic force microscopy (AFM)-based force-spectroscopy experiments we have performed to measure interaction forces between active and inactive 20S proteasomes and a model substrate. The AFM setup used in this study is shown in Fig. 1 *A*. Because of the limited effective cross-section of interaction between the proteasome and the substrate molecules, which is basically determined by the narrow gates in the α-rings, an optimized experimental setup was necessary. This setup relies on a dense and homogeneous immobilization of functional proteasomes in an end-on orientation on a flat support such that the gates in the α-rings are accessible to the substrate (see Fig. 1). The substrate molecules are offered as bait to the proteasomes by binding

Submitted July 8, 2010, and accepted for publication December 2, 2010.
*Correspondence: witt@biochem.mpg.de or baumeist@biochem.mpg.de
Editor: Daniel J. Muller.

0006-3495/11/01/0489/9 $2.00
doi: 10.1016/j.bpj.2010.12.3689

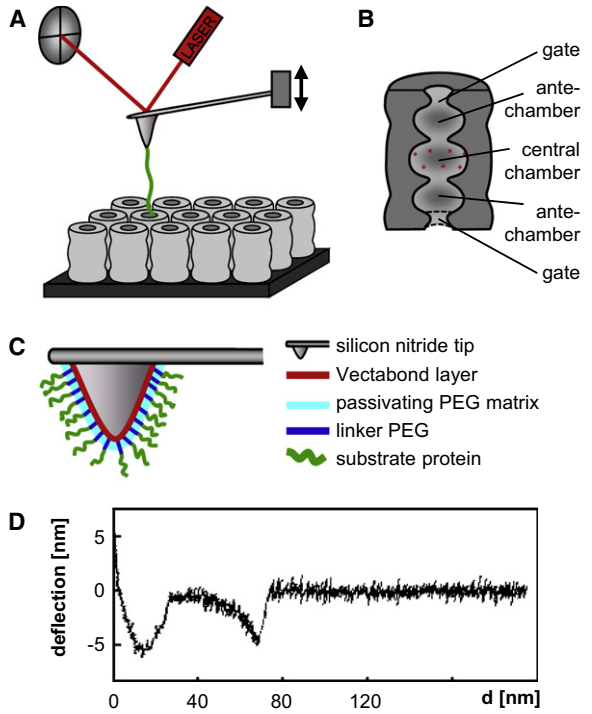

FIGURE 1 Experimental AFM setup, schematic cut-open view of the 20S proteasome, tip functionalization, and exemplary force curve. (*A*) Schematic depiction of the force spectroscopy setup. Proteasomes (shown as *gray cylinders*) are immobilized on mica (*dark gray*) in a dense array in an end-on orientation presenting their pores toward substrate molecules (*green*) that are covalently bound to the tip of a cantilever. A laser beam that is reflected onto a position-sensitive photodiode monitors the cantilever deflection, which is proportional to the force applied to the tip. For conventional force spectroscopy, the cantilever is lowered until the tip contacts the sample; it then pauses and subsequently is retracted. (*B*) Schematic cut-open view of the 20S proteasome showing the location of the gate formed by the outer α-rings, the two antechambers, and the central chamber containing the active sites, depicted in red. (*C*) Schematic representation of a functionalized cantilever tip using a PEG-based approach. (*D*) Representative retraction path of a force-extension curve of a cantilever functionalized according to a PEG-based protocol with casein molecules using immobilized active proteasomes as the sample. The deflection of the cantilever is plotted against the tip-sample distance *d*.

them covalently in a specific orientation to the AFM cantilever tip. As a model substrate, we used two variants of the natively unfolded protein β-casein. These mutants allowed us to address the question as to whether there is a preference for the N- or C-termini of substrates to enter the proteasome first. Using this experimental setup to perform force measurements in two experimental modes, we were able to determine the interaction forces between the 20S proteasome and substrate molecules en route to the active sites.

MATERIALS AND METHODS

Production and purification of recombinant proteins

For the recombinant production of *Methanosarcina mazei* (Mm) 20S proteasomes, we used the active wild type (WT) as well as the inactive active-site mutant (T1A), and two bovine casein mutants (His_6_casein_cysteine (HC) and cysteine_casein_His_6 (CH) in *Escherichia coli* standard isopropyl β-D-thiogalactopyranoside-inducible T7-promoter pET-expression systems. All proteins were purified via a His-tag-based affinity chromatography step followed by a size-exclusion chromatography step. All chromatography runs were performed according to standard protocols. Casein was purified under denaturing conditions. Details about the cloning, expression strategy, and purification scheme are given in the Supporting Material.

AFM

Imaging and force spectroscopy were performed with a NanoScope Multimode IIIa (Digital Instruments, Santa Barbara, CA) in a commercial glass fluid cell. The NanoScope was equipped with a signal access box (Digital Instruments). Images and force curves were recorded using the NanoScope software.

For imaging, we used short, triangular OMCL-TR800 cantilevers (Olympus, Japan; http://probe.olympus-global.com) with a nominal force constant of 0.57 N/m. Imaging was performed in tapping mode in buffer A (10 mM Hepes, 150 mM NaCl, pH 7.5) at tapping amplitudes of 2–3 nm. The resonance frequency was determined from thermal noise spectra in buffer solution to be 23.9 kHz. The excitation frequency was chosen at 17–20 kHz.

Sample preparation

We applied 30 μl of the proteasome sample, dissolved in buffer A containing 20 μg proteasomes, to freshly cleaved mica discs (6 mm in diameter). The conditions for incubation were chosen to achieve the highest occupancy and most evenly distributed coverage of proteasomes on mica. In the case of the WT sample, the solution was incubated for 10 min, whereas the T1A mutant was incubated for 30 min before the sample was thoroughly rinsed with buffer A.

Cantilever functionalization

For the force-spectroscopy experiments, we used two types of cantilevers: a BioLever (Olympus) with a gold-coated tip (nominal force constant 6 pN/nm), and an OMCL-TR-400-PSA (Olympus) with a long triangular cantilever and an SiN tip (nominal force constant 20 pN/nm). The BioLever has higher force sensitivity because of its lower force constant. Both types of cantilevers were functionalized with casein as a substrate protein, according to two different protocols.

Functionalization via thiol-Au bonds

The BioLevers with gold-coated tips were cleaned under UV light for 15 min, incubated in casein (HC) solution (0.8 μg/μl in 4 M urea) for 30 min, and washed several times in buffer A. For passivation, the cantilevers were treated with 50% mercaptoethanol solution in buffer B (20 mM Hepes, 150 mM NaCl, pH 8.4) before and after incubation in the casein solution. In a final step, the functionalized cantilevers were washed in buffer A to remove the excess of protein.

PEG-mediated functionalization

The functionalization protocol we used for the SiN tips of the OMCL-TR-400-PSA cantilevers is based on the method described by Geisler et al. (18). Fig. 1 *C* shows a schematic representation of the tip structure after this functionalization. The cantilevers were cleaned by UV light for 15 min and then treated in a plasma cleaner for 5 min. The SiN surface was then oxidized by incubating the levers for 15 min in RCA solution (10 ml deionized water, 2 ml H_2O_2, 2 ml NH_4OH) at 75°C. Subsequently, the cantilevers were incubated in acetone for 5 min, treated with Vectabond solution (Vector

Laboratories, Burlingame, CA) according to the manufacturer's manual, and immersed in deionized water. NHS-PEG-CH_3O (2000 Da; Rapp Polymere, Tübingen, Germany) and Malhex-NH-PEG-NHS (3000 Da; Rapp Polymere) were dissolved in DMSO to a concentration of 100 μg/μl and 50 μg/μl, respectively. Aliquots were sealed under N_2 and stored at −20°C. The cantilevers were incubated for 2 h in a mixture of 180 μl 100 μg/μl NHS-PEG-CH_3O and 2 μl 50 μg/μl Malhex-NH-PEG-NHS dissolved in 8 ml buffer B. The different lengths of the two PEG molecules (~14 nm for the NHS-PEG-CH_3O vs. ~22 nm for the Malhex-NH-PEG-NHS) ensured that the substrate molecules that were bound to the Malhex-NH-PEG-NHS layer would subsequently protrude from the passivating NHS-PEG-CH_3O layer. Two variants of casein were bound to the maleimide groups of the Malhex-NH-PEG-NHS via the cysteine residues that were introduced at the N- or C-terminal end of casein. N-terminal binding of casein was performed by immersing the cantilevers in a diluted solution of His_6_casein_cysteine (HC) (280 μl buffer B, 35 μl of 4 μg/μl HC in 4M Urea) for 120 min. C-terminal binding of casein was performed by immersing the cantilevers in a diluted solution of cysteine_casein_His_6 (CH; 250 μl buffer B, 40 μl of 1.2 μg/μl CH in 4 M Urea) twice for 120 min. The functionalized cantilevers were washed in 2 M GuHCl, 20 mM Hepes, pH 7.4, and then washed in 2 M NaCl, 20 mM Hepes, pH 7.4, and buffer A to remove excess protein.

AFM force spectroscopy

All force-spectroscopy experiments were performed with the use of an atomic force microscope located in an air-conditioned room. No further temperature regulation was implemented, because the activity levels of archaeal proteasomes at temperatures between 20°C and 40°C are low and of the same order of magnitude (see Fig. S1 and Fig. S2 in the Supporting Material). All experiments were performed in buffer A. Force constants were determined by evaluating the thermal noise spectra (19) and considering corrections for the cantilever shape (20) and tilt (21). Two types of cantilevers were used. As described above, each cantilever was used for a specific functionalization protocol and the respective experimental procedure for the force-spectroscopy experiments.

The force constant of the OMCL-TR-400-PSA cantilevers was determined for each cantilever after use in the force-spectroscopy measurements, resulting in values between 28 pN/nm and 69 pN/nm. This wide range of force constants is caused by partial spalling of the gold coating from the backside of the cantilevers, which occurs during functionalization. The force constant of the BioLever was determined twice per batch. Both measurements resulted in 6 pN/nm.

Conventional force-spectroscopy procedure

Using PEG-functionalized AFM tips, we performed a conventional force-spectroscopy procedure consisting of an approaching path, a time period during which the cantilever tip was in contact with the sample, and a subsequent retraction path. In the relaxed state of the cantilever, no force is applied. The deflection of the cantilever, which depends on external factors and therefore occurs even at large distances from the sample surface, functions as a reference while the sample is approached. All force curves are corrected for the deflection that characterizes the relaxed state of the cantilever. A positive cantilever deflection of 5–10 nm, which indicates tip-sample contact, triggers the arrest of the cantilever in this position for a period of 4 s. This period represents the optimal time for detecting a maximal number of single-molecule events while also detecting only minor numbers of multiple interactions, and ensuring that the overall time required for the series of experiments is still feasible.

During the subsequent retraction of the cantilever, its deflection, representing the corresponding force curve, was recorded. An exemplary force curve is shown in Fig. 1 *D*. All curves were measured under the same conditions (*z*-range and speed were kept constant at values of 200 nm and 400 nm/s, respectively). After each approach procedure, either the x- or y-position of the sample was changed by 200 nm to avoid reexploring the same sample spot. The x- and y-movements were controlled by external voltages fed into the accordingly modified NanoScope controller.

Three-step procedure

When using the BioLever cantilever, we followed a newly developed, three-step procedure (see Fig. 3): Before recording the actual force curves, we determined the approximate *z*-position of the sample surface. We then recorded three successive force curves with a fixed scan range of 200 nm. The *z*-position at which the approach of the first step starts (the surface detection step) was chosen such that a positive cantilever deflection of 5–10 nm was achieved at the point at which the cantilever movement changed from approaching to retracting (reversal point). To avoid contact between the tip and the sample surface during the next step (the measurement step), we started the approach 20 nm farther away from the sample than the first step, resting at the reversal point for 5 s. The increase of 20 nm in distance to the sample was achieved by adding an external voltage to the *z*-drive voltage via the *z*-mod input in the signal access box. In the third step of the procedure (the reevaluation step), we started the cantilever at the initial *z*-position of the first step to detect drift that might have caused unwanted tip-sample contact during the measurement step. Because the noise level of the cantilever deflection signal when the tip is in contact with the sample depends on the nature of the sample surface, we used this noise signal to distinguish between events in which the tip was in contact with mica or with proteasomes on mica.

Evaluation of force curves

Force curves that exhibited the typical shape of the deflection signal of the cantilever corresponding to the elastic stretching of a single polypeptide chain, which can be described by the worm-like chain model (22,23), were selected manually and further analyzed using the software packages MATLAB (The MathWorks, Natick, MA) and IGOR (WaveMetrics, Portland, OR). A typical single-molecule event is shown in Fig. 1 *D* in the region between 40 and 70 nm. We evaluated all curves that showed single-molecule events in the region beyond 25 nm by converting the cantilever deflection at the point of rupture into force values using Hooke's law. Histograms of these force values were fitted with Gaussian distributions. This approximation is valid for the kind of data measured here. The errors given for the center forces of the Gaussian distributions represent a statistical estimate of the standard deviation of the center position.

RESULTS AND DISCUSSION

Experimental setup

To determine the forces involved in the translocation of polypeptide chains into the interior of the 20S complex, we used AFM in the experimental setup described in Fig. 1. The 20S proteasomes were densely and homogeneously immobilized on a flat support in an end-on orientation, which made their pores accessible to substrate molecules that were bound covalently to the tip of the AFM cantilever.

We used 20S proteasomes from the archaeon *M. mazei* for this study because they tend to bind to the mica surface in an end-on orientation. This is simpler and more reliable than the commonly used method to bind His-tagged proteins on functionalized lipid layers, as previously described for the 20S proteasome from *Thermoplasma acidophilum* (24).

Fig. 2 shows representative topographic AFM images of a WT *Methanosarcina* proteasome (Fig. 2 *A*) and an inactive mutant T1A (Fig. 2 *B*) on mica forming dense arrays in

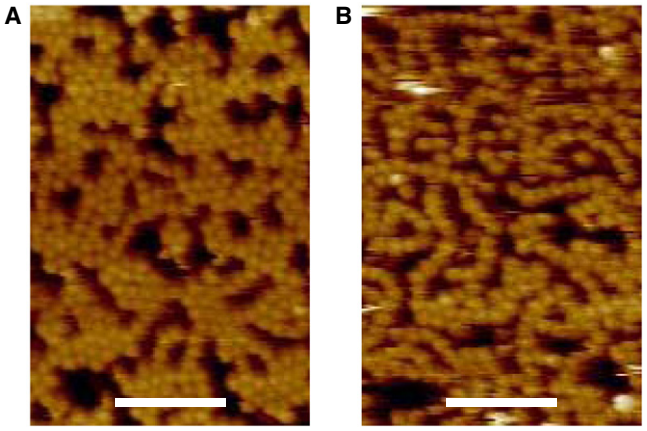

FIGURE 2 Topographical AFM images of active WT (*A*) and inactive active-site mutant (*B*) proteasomes immobilized on mica (scale bar: 100 nm).

end-on orientation. The orientation of the immobilized proteasomes can be concluded from the determined height of ~17 nm and the circular shape corresponding to the top view of the molecules. Although the coverage of the WT and the mutant proteasome seems to differ slightly in the resulting pattern, the overall occupancy is comparable. In both cases, the proteasomes covered 30–40% of the entire support area. Because substrate molecules have to pass a gate that represents <2% of the entire surface area of the top of the proteasome, such a high occupancy is most helpful for force-spectroscopy measurements.

Enzymatic analyses with a variety of substrates have shown that WT *Methanosarcina* proteasomes are active in solution as well as after immobilization (see Fig. S2). The reduction in activity when the proteasomes are immobilized on mica compared with their activity in solution is consistent with the model in which full activity can only occur when both gates are accessible for substrate molecules to enter the 20S proteasomes (25).

The natively unfolded conformation of casein makes it a suitable substrate molecule (26). Because casein lacks a tightly folded core domain, its behavior in solution is comparable to that of a flexible spring and can be described by the worm-like chain model (22,23). By estimating from the number of amino acid residues and a well-established value for the length of a peptide bond (27), we determine the contour length of casein to be 72 nm. In our force-spectroscopy studies, we determined the persistence length of casein to be 0.5 nm. Using the described values for persistence length and contour length, we calculate a probability of 24% that the end-to-end distance for β-casein in buffer is larger than 10 nm at a given time point (data not shown). Here, we define a single-molecule event as an interaction event that involves only one substrate molecule and can easily be recognized by the typical shape of the respective force curve (see Figs. 1 *D* and 3 *C*, and Fig. S3, *B–D*). The elastic stretching of one polypeptide during retraction

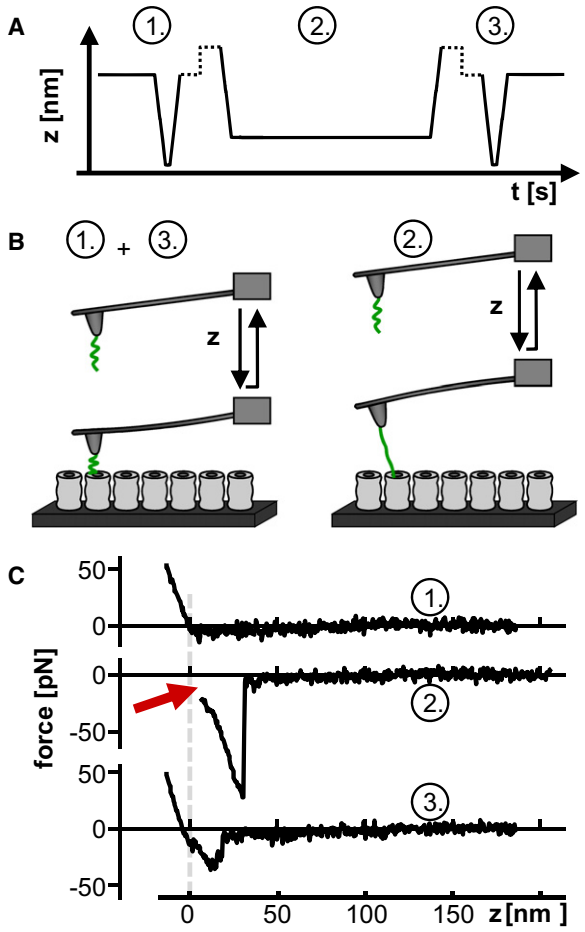

FIGURE 3 Schematic representation of the three-step procedure and direct visualization of substrate translocation. (*A*) The cantilever position *z* during the three successive approach curves of the three-step procedure (step 1: surface detection; step 2: measurement; step 3: reevaluation) is depicted with respect to the sample position over time. (*B*) Schematic representation of the corresponding experimental procedure showing the stretching state of the substrate molecule (*green*) and the corresponding bending of the cantilever. (*C*) Retraction paths of three successive force curves according to the three-step procedure performed with casein HC and active WT proteasomes. The *z*-position of the sample surface is determined in the first step and depicted as a dashed line. The retraction path of the measurement step starts with a negative deflection of 3.5 nm of the cantilever corresponding to a force of 21 pN at a distance of 8 nm above the sample surface (*red arrow*).

of the cantilever causes an arching of the force curve that ends in a sudden jump back into a zero force (the relaxed state of the cantilever) due to the rupture of this interaction. The distance between the rupture point and the contact point (i.e., the rupture distance) is used during evaluation of conventional force-spectroscopy experiments as a criterion to reject all events with a rupture distance < 25 nm. Cases in which this distance is smaller than the threshold could be dominated or at least influenced by nonspecific tip-sample interactions. Simultaneous multiple interactions by casein are easily detected because these interactions will rupture at several different points in the force curve. In

practice, such multiple interactions are rare because only a few of the many substrate molecules bound to the cantilever tip can reach the sample surface, due to the cone-like shape of the tip, and in addition the effective interaction cross-section of the proteasome's pore is very limited.

Two different protocols for the covalent linkage of casein molecules to the AFM cantilever tip were used. Both protocols are based on the chemical binding of a cysteine residue introduced by mutation into the casein molecule to a suitably coated AFM tip.

One approach was to bind casein via a covalent thiol-Au bond mediated by a terminal cysteine. The gold-coated BioLever, to which casein can be bound directly, has high force sensitivity. Any analysis of data obtained with a functionalized BioLever will be hampered by frequently occurring signals originating from nonspecific tip-sample interactions that interfere with signals resulting from substrate-sample interactions. However, we were able to use the BioLever to perform specific force-spectroscopy measurements. Our complex, three-step procedure allowed us to record force spectra while avoiding direct tip-sample contact. This three-step procedure is described in more detail below.

In a second approach, we were able to improve the specificity of tip-sample interactions by establishing a PEG-based binding procedure for the substrate molecules via their terminal cysteine residues to SiN tips. The multistep functionalization scheme of the AFM cantilever tip is depicted in Fig. 1 *C*. In comparison with the gold-coated tips, the unspecific adhesion of the tip to the sample is much reduced by the PEG layer. As can be seen in Fig. 1 *D*, the interactions between the proteasomes and the functionalized cantilever tip can be separated into two parts: During retraction of the tip from the sample, the interaction signature of the sample with the PEG matrix can often be observed up to a distance of ~25 nm. This distance corresponds to the thickness of the PEG layer. Forces observed during further retraction of the AFM tip indicate interactions between sample and substrate molecules, as these are the only molecules protruding out of the PEG layer. Further examples of such force curves recorded using PEG-functionalized SiN tips are shown in Fig. S3.

To ensure the accuracy of the interpretation of force curves taken with the functionalized PEG tips, we performed several control experiments. We did not detect a single-molecule event with a rupture distance of >25 nm in any of the ~1200 recorded force curves derived from experiments in which bare mica was approached by substrate-loaded PEG tips. Single-molecule events occurred only in experiments in which proteasomes were immobilized on mica. Further force control curves were recorded using the PEG tip before functionalization with substrate molecules and compared with those recorded after functionalization. Single-molecule events were observed in ~4.4% of all experiments performed with casein-loaded PEG tips and proteasomes immobilized on mica as the sample. Surprisingly, single-molecule events were also detected when PEG tips without any substrate molecules attached were used. However, we observed such single-molecule events in only five of 965 approach curves using immobilized active proteasomes in a substrate-free context. Such events could arise from mechanical unfolding of individual proteasome subunits picked up by the AFM cantilever tip, or even from detachment of single subunits from the proteasome by the tip. Interactions that are not based on the interplay between proteasome and substrate molecules contribute only ~10% to the total number of single-molecule events analyzed, and scatter between 20 and 200 pN. Hence, such events represent a negligible background to the interaction forces of interest. Multiple single-molecule events within one force curve were rare and could be separated during the evaluation process.

Altogether, we recorded more than 15,000 conventional force curves using fully functionalized PEG tips and immobilized proteasomes as the sample. In accordance with the described validation procedure, we can attribute the observed single-molecule events to interactions between the immobilized proteasomes and the substrate molecules covalently bound to the AFM tip.

Detection of active substrate translocation events using the three-step procedure

We have developed a method involving three successive approach procedures (Fig. 3) for data acquisition that allows an unambiguous and direct determination of specific proteasome-substrate interaction events. This method ensures that the tip does not make contact with the sample while the force curve representing the actual measurement step is being recorded. Therefore, it is very likely that rupture events detected during this step result from the interaction between proteasomes and substrate molecules protruding from the AFM cantilever tip. This procedure is especially valuable when nonspecific tip-sample interactions dominate, as described above for the gold-coated BioLever. Moreover, the three-step procedure allows the detection of events during which the functionalized tip is actively pulled toward the sample. It is not possible to detect such events, which can be interpreted as active substrate translocation events (as outlined below), using conventional force-spectroscopy protocols. Fig. 3 *C* shows an example of this rare event, obtained using our three-step procedure. The force curve recorded during the second measurement step exhibits the typical signal shape of a single-molecule event that can be attributed to casein interacting with a proteasome and therefore being stretched during the retraction path of the AFM tip. Of interest, the AFM cantilever is already in a state of negative deflection corresponding to an attractive force of 21 pN when retraction of the cantilever is initiated. Drift during the whole measurement can be excluded, as the

contact points in the first and third curves in Fig. 3 *C* match well. This absence of drift guarantees that in the second step the tip surface and sample did not come into contact while the tip resided close to the sample during the several seconds of resting time preceding retraction. This allows us to conclude that a single casein molecule was actively pulled toward or into a proteasome against the spring force of the resting cantilever. Of interest, so far, we have observed such events occurring with the cantilever being in a state of negative deflection before initiating the retraction only in the case of active proteasomes. The set of force curves shown in Fig. S4 includes an event-free curve followed by curve in which a single-molecule event can be detected that is not preceded by an active pulling event. Although this highly specific three-step procedure offers advantages over conventional force-measurement protocols, the efficiency of the method, which currently is reproducible below 1%, needs to be improved. Moreover, alterations of the current setup that would allow continuous recording of the deflection signal, as well as automatization of the procedure, would ultimately enable direct monitoring of substrate translocation.

Directional specificity of the proteasome-substrate interactions

Despite the need for a more complex functionalization scheme when binding the substrate molecules via PEG linkers to passivated tips, we chose to use this approach for systematic studies on the forces occurring during the translocation into 20S proteasomes. The passivation of the AFM tips suppresses nonspecific tip-sample interactions effectively, thus facilitating force spectroscopy experiments with a higher throughput. To test whether the proteasome preferably interacts with a specific terminus of the substrate molecules, we engineered two variants: HC and CH. Because of the antipodal position of the tags, these casein mutants can be bound to the cantilever in opposite orientations, allowing only interactions of the proteasome with either the N- or C-terminus of the casein molecules. Tips that were functionalized with either of the casein mutants (HC or CH), according to the PEG-based binding procedure described in Fig. 1 *C*, were used in force measurements on immobilized WT 20S proteasomes and immobilized inactive Thr1Ala mutant proteasomes. For each of the four combinations of the described proteasome and casein mutants, a set of at least 3000 conventional force curves was recorded. Each set was recorded during six to eight individual sessions. The frequency of identified single-molecule events varied slightly from 4.0 ± 0.4% and 4.1 ± 0.3% when determining the forces exerted on the C-terminus of the casein molecules by the inactive and active proteasome, respectively, to 4.7 ± 0.3% and 4.6 ± 0.3% when determining the forces exerted on the N-terminus of the casein molecules. However, the difference in the frequency of analyzed single-molecule events is within the standard variation and therefore is not statistically significant. The values for the interaction forces determined in the described experiments scatter around the mean values, as expected for a statistical process influenced by thermal energy (28,29). The histograms of these forces are given in Fig. 4 *A*. The overall distribution function of occurring forces in each set of experiments is mirrored in all sessions of this set. No significant difference in the distribution of the interaction forces between the two casein mutants could be detected for the active WT or the inactive proteasome mutant (Fig. 4 *B*). Therefore, we conclude that the 20S proteasome has no preference for the N- or C-terminal

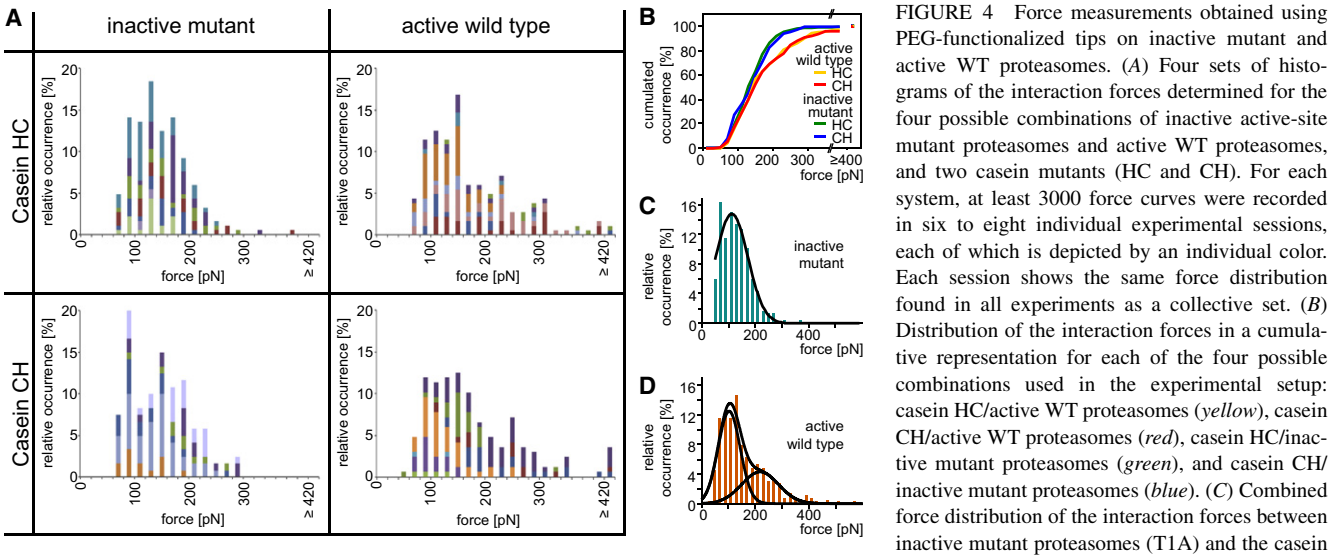

FIGURE 4 Force measurements obtained using PEG-functionalized tips on inactive mutant and active WT proteasomes. (*A*) Four sets of histograms of the interaction forces determined for the four possible combinations of inactive active-site mutant proteasomes and active WT proteasomes, and two casein mutants (HC and CH). For each system, at least 3000 force curves were recorded in six to eight individual experimental sessions, each of which is depicted by an individual color. Each session shows the same force distribution found in all experiments as a collective set. (*B*) Distribution of the interaction forces in a cumulative representation for each of the four possible combinations used in the experimental setup: casein HC/active WT proteasomes (*yellow*), casein CH/active WT proteasomes (*red*), casein HC/inactive mutant proteasomes (*green*), and casein CH/inactive mutant proteasomes (*blue*). (*C*) Combined force distribution of the interaction forces between inactive mutant proteasomes (T1A) and the casein mutants HC and CH. The histogram can be described by one Gaussian distribution, depicted as a black line. (*D*) Combined force distribution of the interaction forces between active WT proteasomes and the casein mutants HC and CH. The histogram can be described by the sum of two individual Gaussian distributions, depicted as black lines.

end of a substrate molecule. Of course, the situation could change in cases in which the 20S proteasome acts on a substrate in conjunction with a regulatory complex involved in the unfolding and translocation of substrates.

For the 26S proteasome, investigators have suggested two alternative models in which it is assumed that the degradation of substrate molecules is initiated at one terminus (30) or at an internal site (31,32). Initiation of substrate degradation at an internal site requires threading of a loop region of the substrate molecule into the proteolytic chamber, where the substrate has to be processed endoproteolytically. Such activity was elegantly shown for the proteasome by Liu et al. (33) using artificial circular substrates. Subsequent complete degradation of the substrate molecules can only occur if the proteasome is able to process the substrate from the N-terminus as well as from the C-terminus onward (34). The data presented here suggest that the 20S proteasome itself does not show a clear preference for one or the other terminus of an unfolded substrate. Because both constructs are His-tagged on the opposite end to the cysteine mutation, we cannot exclude the possibility that a preference of the proteasome for this sequence tag obscures a terminus-specific preference; however, to our knowledge, no such sequence preference has been reported. The ability of a bidirectional degradation of the 20S proteasome would be advantageous for an efficient degradation of unfolded proteins.

Stability of proteasome-substrate interactions

Fig. 4, *C* and *D*, show the histograms of forces determined for the interaction between casein and the inactive mutant as well as the active WT proteasome. Based on the finding that neither the active nor the inactive proteasome used in the described force experiments exhibits significantly different forces when interacting with the N- or C-terminus of casein, we conclude that the results for the two experimental sets can be jointly considered. The force distribution in the histogram of the inactive proteasomes can be approximately described by one Gaussian distribution that centers around 113 $\pm$ 4 pN. The width of this distribution is 85 $\pm$ 6 pN. The histogram of the active proteasomes is asymmetric and reaches higher forces: ~20% of the events occur at forces above 220 pN, whereas $<$3% do so in the case of the inactive proteasomes. Thus, the histogram of the active proteasomes is better described by two Gaussian distributions centered at 103 $\pm$ 6 pN and 220 $\pm$ 40 pN. The widths of these distributions are 58 $\pm$ 8 pN and 97 $\pm$ 41 pN, respectively. Another approach to describe the histogram of the active proteasomes is to define the center of the low force peak by the value of 113 pN as determined for inactive proteasomes. The high force peak resulting from this approach centers around 250 $\pm$ 10 pN. The widths of these distributions are 67 $\pm$ 7 pN and 59 $\pm$ 14 pN. Both approaches result in virtually the same values for the maxima within the error margins. However, the quality of the fit is lower when the low force peak is defined at 113 pN.

By separating the force distribution in the case of the active proteasomes (Fig. 4 *D*) into two Gaussian distributions, we can assign 65% of all events to the low force distribution and 35% to the high force distribution. The distribution of the interaction forces determined for the inactive mutant is virtually identical to the low force peak of the distribution of the WT interaction forces.

Mutation of the active-site residue threonine to alanine leads to a proteasome mutant that is unable to process any peptide bonds, including that of its own propeptide. Structural studies have shown that the presence of the propeptides changes the conformation of the active sites and their neighboring environment (35), which traps the proteasome in an inactive state. Because propeptide added in trans does not inhibit the proteasome, it is likely that the difference in the force distribution is related to the altered conformation of the active site and its surrounding active cleft. This raises the question as to how the difference in the conformation of the active site clefts located in the central chamber of the proteasome can cause such a change in proteasome-substrate interaction forces. Forces in the range found in this study were previously reported for the rupture of intramolecular interactions during the unfolding of titin domains (36), as well as for the rupture of intermolecular interactions in the biotin-avidin system (37). Forces in this range can be attributed to the rupture of multiple electrostatic interactions. This allows the assumption that a variety of hydrogen- and salt-bridges are formed, which then mediate the interaction of substrate molecules with the proteasome. Furthermore, the data presented here allow the conclusion that the formation of such interactions between the proteasome and a substrate molecule, in the range of 100 pN, are independent of the ability of the proteasome to degrade the substrate molecules. Such interactions must relate to the specific architecture of the proteasome. In principle, the substrate can interact with residues on the outside of the proteasome, within the gate, or with residues lining the passageway from the gate to the central cavity. These residues represent sites a substrate must pass to reach the active sites where proteolysis takes place. The total yields of interaction events observed for the WT and the inactive mutant proteasome were virtually identical: 4.3 $\pm$ 0.2% for the WT vs. 4.4 $\pm$ 0.3 for the mutant. This means that in both cases, specific interactions between casein and the two proteasome types occur with the same probability. This allows the conclusion that the fraction (35%) of all events that occur in the case of the inactive mutant at low interaction forces occurs at higher interaction forces in the case of the active WT. Because the major difference between active and inactive proteasomes is alterations of the active clefts in the central chamber, it is reasonable to assume that at least this 35% of all events must be based on interactions with residues of the central chamber. This means that at least

parts of the substrate molecule must have entered the proteasome, and thus it seems reasonable to attribute the remaining 65% of events occurring at interaction forces in the range of 100 pN observed for active and inactive proteasomes to the process of substrate translocation en route to the central chamber. Such an interpretation would mean that proteasomes are able to translocate substrate molecules independently of their processing.

For translocation, the proteasome must strike the right energetic equilibrium of interactions with the substrate molecules to ensure substrate binding and substrate mobility. Once the substrate has approached the central chamber, stronger interactions can take place, as depicted in Fig. 5.

The increase in the stability of the interaction between the proteasome and the substrate in WT proteasomes could reflect a structural change in the proteasome's interior induced by the presence of the substrate. However, the nature of this increase remains unclear. Because casein exists in an unfolded state, and proteasomes can degrade any protein that is unfolded and capable of entering the central cavity, it is very unlikely that a conformational change of the substrate is responsible for the observed increase in interaction forces. A more likely explanation would be a stronger interaction of the substrate with the active-site cleft in the WT than in the inactive active-site mutant proteasome, or some collective changes in its interior that occur upon binding of the substrate to the active-site cleft. The fact that crystal structures of proteasomes with and without inhibitors bound have not revealed larger conformational changes suggests that such conformational changes, if they occur, have a dynamic character.

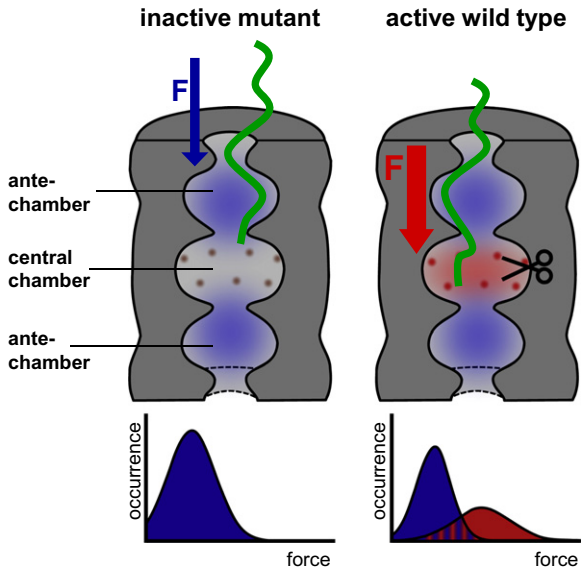

FIGURE 5 Interactions between the proteasome and the substrate promote substrate translocation. The forces determined via the force-spectroscopy experiments described in this work can be attributed to interaction events between the substrate protein casein (*green*) and active WT and inactive mutant proteasomes. A comparison of the histograms derived from these interaction forces for active versus inactive proteasomes allows us to conclude that the interactions take place in the interior of the proteasome. One contribution to the interactions must relate to the specific architecture of the proteasomes, providing a basis for capturing substrates with a probability beyond pure diffusion statistics (depicted in *blue*). It is very likely that the observed enhanced interaction forces for the active proteasomes (depicted in *red*) involve amino acid residues located in the central chamber or even the active sites (indicated as *dots* in this figure). This enhanced interaction force may promote directed translocation of the substrate into the central cavity by further net movement of the substrate or by its position in close proximity to the active cleft. The underlying mechanism could be a stronger interaction of the substrate with the active-site cleft in the WT compared with the active-site mutant proteasome, or some collective changes in the interior of the proteasome that occur upon binding of the substrate to the active-site cleft, possibly by an allosteric mechanism. One may even hypothesize that the degradation activity itself induces conformational changes that enhance the interaction force.

CONCLUSIONS

The above uncertainties in interpretation notwithstanding, the force-spectroscopy experiments presented here allow us for the first time, to our knowledge, to determine the forces of interaction events related to the translocation of substrate molecules into the 20S proteasome. By performing a variety of force-spectroscopy experiments, we are able to clarify the ability of the proteasome to interact with substrates in a bidirectional manner, i.e., without a significant preference for the N- or C-terminus. The results also indicate that the ability of the proteasome to process substrate molecules induces a switch from one state of the proteasome to another in which stronger interactions with the substrate molecule can be formed, stabilizing the interaction once the substrate has reached the central cavity.

SUPPORTING MATERIAL

Details about the cloning, expression strategy, and purification scheme, and four figures and references are available at http://www.biophysj.org/biophysj/supplemental/S0006-3495(10)05202-1.

This work was supported by the Deutsche Forschungsgemeinschaft (SFB 486 and 594)

REFERENCES

1. Ciechanover, A. 1994. The ubiquitin-proteasome proteolytic pathway. *Cell.* 79:13–21.
2. Coux, O., K. Tanaka, and A. L. Goldberg. 1996. Structure and functions of the 20S and 26S proteasomes. *Annu. Rev. Biochem.* 65:801–847.
3. Baumeister, W., J. Walz, …, E. Seemüller. 1998. The proteasome: paradigm of a self-compartmentalizing protease. *Cell.* 92:367–380.
4. Finley, D. 2009. Recognition and processing of ubiquitin-protein conjugates by the proteasome. *Annu. Rev. Biochem.* 78:477–513.
5. Löwe, J., D. Stock, …, R. Huber. 1995. Crystal structure of the 20S proteasome from the archaeon *T. acidophilum* at 3.4 A resolution. *Science.* 268:533–539.
6. Groll, M., M. Bajorek, …, D. Finley. 2000. A gated channel into the proteasome core particle. *Nat. Struct. Biol.* 7:1062–1067.

7. Denny, J. B. 2004. Growth-associated protein of 43 kDa (GAP-43) is cleaved nonprocessively by the 20S proteasome. *Eur. J. Biochem.* 271:2480–2493.
8. Akopian, T. N., A. F. Kisselev, and A. L. Goldberg. 1997. Processive degradation of proteins and other catalytic properties of the proteasome from *Thermoplasma acidophilum*. *J. Biol. Chem.* 272:1791–1798.
9. Dolenc, I., E. Seemüller, and W. Baumeister. 1998. Decelerated degradation of short peptides by the 20S proteasome. *FEBS Lett.* 434:357–361.
10. Dick, T. P., A. K. Nussbaum, …, H. Schild. 1998. Contribution of proteasomal β-subunits to the cleavage of peptide substrates analyzed with yeast mutants. *J. Biol. Chem.* 273:25637–25646.
11. Nussbaum, A. K., T. P. Dick, …, H. Schild. 1998. Cleavage motifs of the yeast 20S proteasome β subunits deduced from digests of enolase 1. *Proc. Natl. Acad. Sci. USA.* 95:12504–12509.
12. De Mot, R., I. Nagy, …, W. Baumeister. 1999. Proteasomes and other self-compartmentalizing proteases in prokaryotes. *Trends Microbiol.* 7:88–92.
13. Holzhütter, H. G., and P. M. Kloetzel. 2000. A kinetic model of vertebrate 20S proteasome accounting for the generation of major proteolytic fragments from oligomeric peptide substrates. *Biophys. J.* 79:1196–1205.
14. Kuttler, C., A. K. Nussbaum, …, K. P. Hadeler. 2000. An algorithm for the prediction of proteasomal cleavages. *J. Mol. Biol.* 298:417–429.
15. Luciani, F., C. Keşmir, …, R. J. de Boer. 2005. A mathematical model of protein degradation by the proteasome. *Biophys. J.* 88:2422–2432.
16. Peters, B., K. Janek, …, H. G. Holzhütter. 2002. Assessment of proteasomal cleavage probabilities from kinetic analysis of time-dependent product formation. *J. Mol. Biol.* 318:847–862.
17. Zaikin, A., and J. Kurths. 2006. Optimal length transportation hypothesis to model proteasome product size distribution. *J. Biol. Phys.* 32:231–243.
18. Geisler, M., T. Pirzer, …, T. Hugel. 2008. Hydrophobic and Hofmeister effects on the adhesion of spider silk proteins onto solid substrates: an AFM-based single-molecule study. *Langmuir.* 24:1350–1355.
19. Hutter, J. L., and J. Bechhoefer. 1993. Calibration of atomic-force microscope tips. *Rev. Sci. Instrum.* 64:1868–1873.
20. Stark, R. W., T. Drobek, and W. M. Heckl. 2001. Thermomechanical noise of a free v-shaped cantilever for atomic-force microscopy. *Ultramicroscopy.* 86:207–215.
21. Hutter, J. L. 2005. Comment on tilt of atomic force microscope cantilevers: effect on spring constant and adhesion measurements. *Langmuir.* 21:2630–2632.
22. Bustamante, C., J. F. Marko, …, S. Smith. 1994. Entropic elasticity of λ-phage DNA. *Science.* 265:1599–1600.
23. Marko, J. F., and E. D. Siggia. 1995. Stretching DNA. *Macromolecules.* 28:8759–8770.
24. Thess, A., S. Hutschenreiter, …, R. Guckenberger. 2002. Specific orientation and two-dimensional crystallization of the proteasome at metal-chelating lipid interfaces. *J. Biol. Chem.* 277:36321–36328.
25. Hutschenreiter, S., A. Tinazli, …, R. Tampé. 2004. Two-substrate association with the 20S proteasome at single-molecule level. *EMBO J.* 23:2488–2497.
26. Chakraborty, A., and S. Basak. 2007. pH-induced structural transitions of caseins. *J. Photochem. Photobiol. B.* 87:191–199.
27. Ainavarapu, S. R. K., J. Brujic, …, J. M. Fernandez. 2007. Contour length and refolding rate of a small protein controlled by engineered disulfide bonds. *Biophys. J.* 92:225–233.
28. Evans, E., and K. Ritchie. 1997. Dynamic strength of molecular adhesion bonds. *Biophys. J.* 72:1541–1555.
29. Dudko, O. K., G. Hummer, and A. Szabo. 2008. Theory, analysis, and interpretation of single-molecule force spectroscopy experiments. *Proc. Natl. Acad. Sci. USA.* 105:15755–15760.
30. Palombella, V. J., O. J. Rando, …, T. Maniatis. 1994. The ubiquitin-proteasome pathway is required for processing the NF-κ B1 precursor protein and the activation of NF-κ B. *Cell.* 78:773–785.
31. Hoppe, T., K. Matuschewski, …, S. Jentsch. 2000. Activation of a membrane-bound transcription factor by regulated ubiquitin/proteasome-dependent processing. *Cell.* 102:577–586.
32. Rape, M., T. Hoppe, …, S. Jentsch. 2001. Mobilization of processed, membrane-tethered SPT23 transcription factor by CDC48(UFD1/NPL4), a ubiquitin-selective chaperone. *Cell.* 107:667–677.
33. Liu, C.-W., M. J. Corboy, …, P. J. Thomas. 2003. Endoproteolytic activity of the proteasome. *Science.* 299:408–411.
34. Piwko, W., and S. Jentsch. 2006. Proteasome-mediated protein processing by bidirectional degradation initiated from an internal site. *Nat. Struct. Mol. Biol.* 13:691–697.
35. Kwon, Y. D., I. Nagy, …, B. K. Jap. 2004. Crystal structures of the *Rhodococcus* proteasome with and without its pro-peptides: implications for the role of the pro-peptide in proteasome assembly. *J. Mol. Biol.* 335:233–245.
36. Rief, M., M. Gautel, …, H. E. Gaub. 1997. Reversible unfolding of individual titin immunoglobulin domains by AFM. *Science.* 276: 1109–1112.
37. Florin, E.-L., V. T. Moy, and H. E. Gaub. 1994. Adhesion forces between individual ligand-receptor pairs. *Science.* 264:415–417.